Supplementary Information (SI) for Journal of Materials Chemistry A.

Supporting Information

Methylated naphthalene additives with various melting and boiling points enable a win-win scenario of optimizing both cost and efficiency of polymer solar cells

Tao Li [a], Xiaoying Zhang [a], Qi Chen [b], Zhi-Guo Zhang [b], Ping Shen*[a,c], Chao Weng*[a]

[a] Key Laboratory for Green Organic Synthesis and Application of Hunan Province, Key Laboratory of Environmentally Friendly Chemistry and Application of Ministry of Education, College of Chemistry, Xiangtan University, Xiangtan 411105, China.

[b] State Key Laboratory of Chemical Resource Engineering Beijing Advanced Innovation Center for Soft Matter Science and Engineering, Beijing University of Chemical Technology, Beijing 100029, China.

[c] Key Laboratory of Organic Synthesis of Jiangsu Province, College of Chemistry, Chemical Engineering and Materials Science, Soochow University, Suzhou, 215123, China.

*Corresponding author: E-mail: wengc2013@163.com (C. Weng);
shenping802002@xtu.edu.cn (P. Shen); zgzhangwhu@iccas.ac.cn (Z.-G. Zhang)

1. Analytical Instruments

Ultraviolet-visible (UV-vis) absorption spectra were measured on Agilent cary60 spectrometer. The photoluminescence (PL) spectrum was conducted on an HORIBA Instrument QM40. Thermal gravimetric analysis (TGA) was performed under nitrogen at a heating rate of 5 °C min^{-1} with TGA Q50 analyzer. The morphologies of the four blend films were characterized by atomic force microscopy (AFM, Multimode 8 with a tapping mode). Grazing incidence wide angle X-ray scattering (GIWAXS) was performed at 1W1A Diffuse X-ray Scattering Station, Beijing Synchrotron Radiation Facility (BSRF-1W1A), China. The samples were prepared in silicon substrates using identical blend solutions and conditions as those used in device fabrication. The solution of each pure organic material was spin-coated on cleaned ITO substrates. Droplets of two different liquids, water and ethylene glycol (EG) were cast onto the pure organic films with the drop size kept at 1 μL per drop. Contact angle images were taken at 4 s after the whole droplet was deposited onto the sample surface. At least 3 independent measurements were performed for each single liquid.

2. Measurement of hole and electron mobilities

The charge carrier mobilities of the binary active layers were measured by using the space-charge-limited current (SCLC) method. Hole-only devices with a structure of ITO/PEDOT: PSS/active layer/MoO_3/Ag and electron-only devices with a structure of ITO/ZnO/active layer/PFN-Br/Ag were fabricated. The device characteristics were extracted by modeling the dark current under forward bias using the SCLC expression described by the Mott-Gurney law:

$$J = \frac{9}{8}\varepsilon_r \varepsilon_0 \mu \frac{V^2}{L^3}$$

Here, $\varepsilon_r \approx 3$ is the average dielectric constant of blend film, ε_0 is the permittivity of the free space, μ is the carrier mobility, L is the thickness of active layers, and V is the applied voltage.

3. Charge transport, exciton dissociation, and charge collection properties

V_{OC} and P_{light} follow the relationship: $V_{OC} \propto nK_BT/q \ln(P_{light})$, the value of n determines the main charge recombination type of PSCs. J_{SC} and P_{light} satisfy the equation: $J_{SC} \propto P_{ligh}^{\alpha}$, the value of α reflects the strength of bimolecular recombination. J_{ph} satisfies the equation: $J_{ph}=J_L-J_D$, V_{eff} can be defined as $V_{eff}= V_0-V_{appl}$ (J_L and J_D stand for the current density in bright and dark environments, V_0 represents the voltage when the J_{ph} is equal to zero, and the V_{appl} refers to the voltage applied to the device). The exciton dissociation probability (*P(E,T)*) can be acquired from the J_{ph}-V_{eff} curves, and the value of J_{ph}/J_{sat} determines the *P(E,T)*. The charge collection efficiency (P_{Coll}) value is determined by the value J_{max}/J_{sat} (J_{max} is the current density when the device is under the condition of the maximum output power).

4. Supplementary Figures

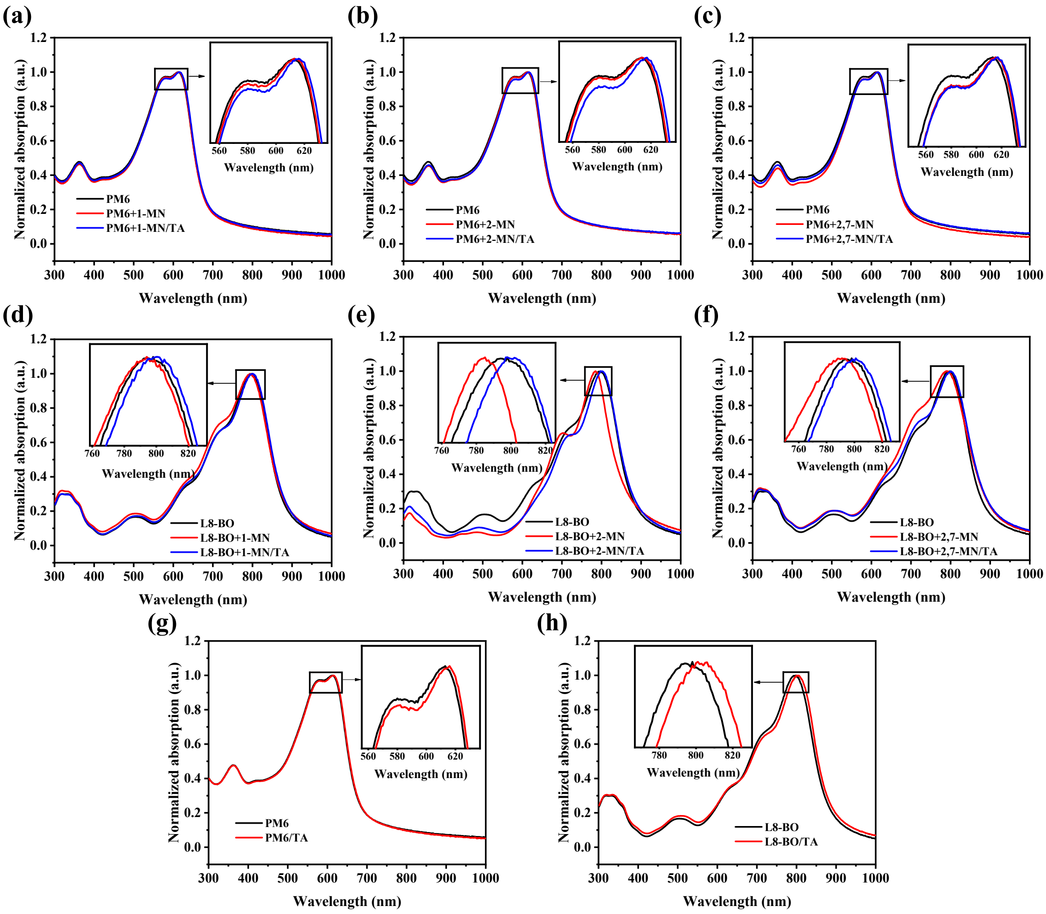

Fig. S1. UV-vis absorption spectra of PM6 film and L8-BO film under different conditions.

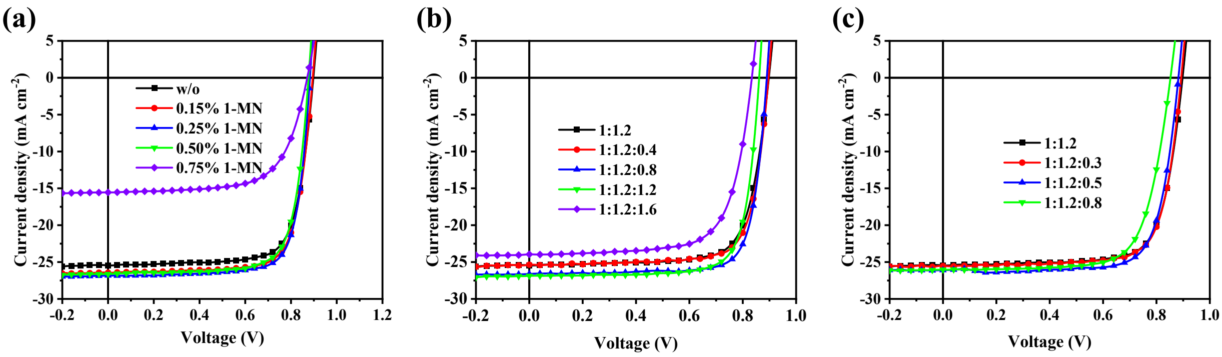

Fig. S2. The *J-V* curves of the device processed with different additive ratio: (a) **1-MN** ratios, (b) **2-MN** ratios, and (c) **2,7-MN** ratios.

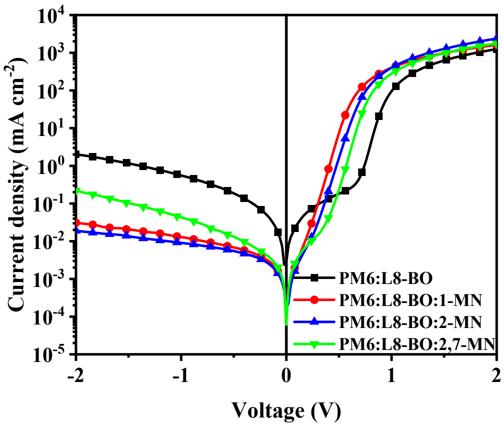

Fig. S3. The dark current curves of the device under different conditions.

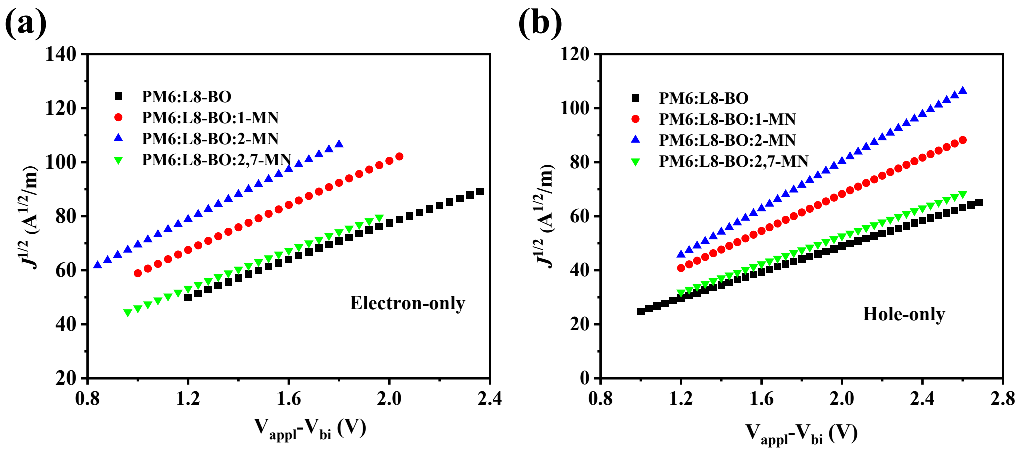

Fig. S4. (a) μ_e and (b) μ_h of the device processed without/with different additives.

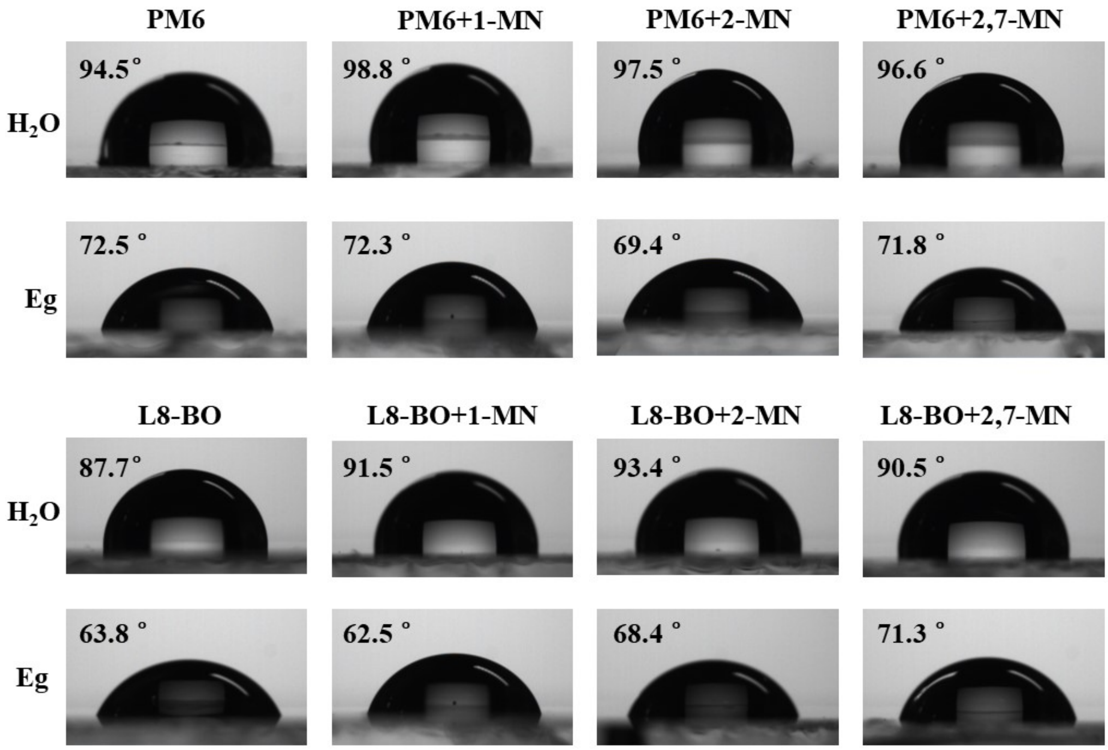

Fig. S5. Contact angles of PM6 and L8-BO films under different conditions.

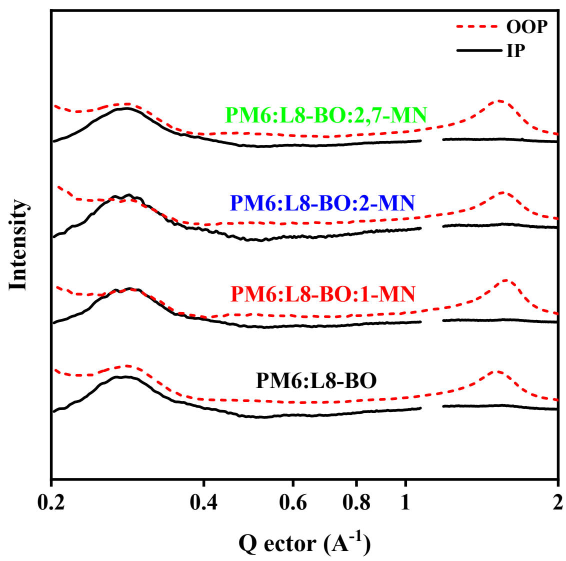

Fig. S6. The OOP and IP line cuts from 2D GIWAXS patterns.

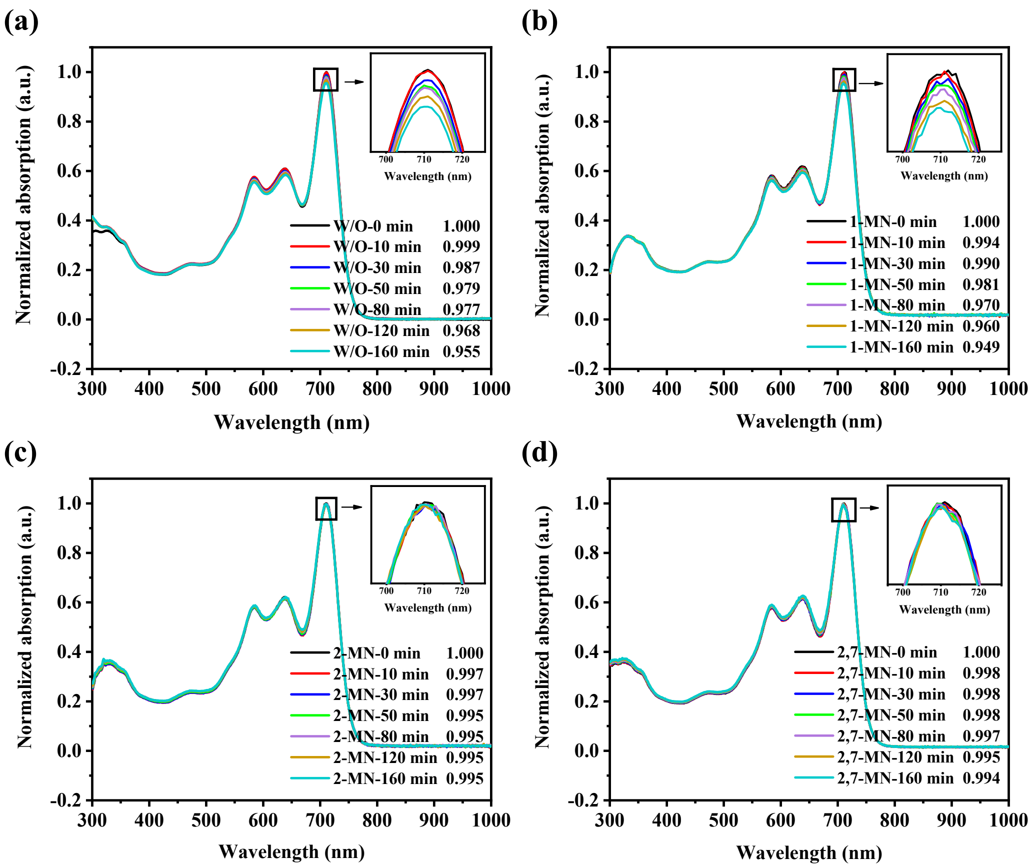

Fig. S7. UV-vis absorption spectra of the PM6/L8-BO blend solution under different conditions.

5. Supplemental Tables

Table S1. The prices of some reported non-halogenated volatile solid additives and corresponding FF and PCE of PSCs.

Additives	Price (from Energy Chemical)	FF [%]	PCE [%]	System	Ref.
NA	￥20/100g	78.42	16.52	PM6:Y6	[1]
2-MON	￥25/25g	76.40	17.32	PM6:PY-DT	[2]
DMON	￥774/25g	59.30	11.19	PBDB-T:TTC8-O1-4F	[3]

BDT	￥4760/5g	77.11	17.91	PM6:Y6	[4]
Ph	￥451/25g	77.82	18.47	D18-Cl:N3	[5]
DBT	￥62/25g	79.33	18.87	PM6:L8-BO	[6]
9-FL	￥25/25g	79.00	18.60	PM6:BTP-eC9	[7]
TT	￥720/25g	75.10	17.75	PM6:Y6	[8]
DTT-3	￥2159/5g	73.60	14.82	PM6:L15	[9]
DOB	￥22/25g	75.60	17.05	PM6:L8-BO	[10]
TMB	￥31/25g	79.95	18.61	PBDB-TF:eC9	[11]
BPO	￥20/25g	70.70	8.03	PTB7:$PC_{71}BM$	[12]
Bipy	￥44/25g	69.44	8.73	J51:N2200	[13]
2T	￥66/25g	78.60	18.10	PM6:Y6	[14]
Fc	￥45/100g	76.00	17.40	PM6:Y6	[15]
TPA	￥39/25g	77.65	17.30	PM6:BTP-eC9	[16]
2-MN	￥30/25g	78.91	18.70	PM6:L8-BO	This work

Table S2. Photovoltaic performance of the device with different **1-MN** ratios.

additive	V_{OC} [V]	J_{SC} [mA cm^{-2}]	FF [%]	PCE [%]
w/o	0.898	25.45	75.08	17.15
0.15%**1-MN**	0.895	26.43	75.83	17.94
0.25%**1-MN**	0.883	26.82	77.22	18.29
0.50%**1-MN**	0.877	26.63	75.41	17.61
0.75%**1-MN**	0.871	15.55	66.91	9.06

Table S3. Photovoltaic performance of the device with different **2-MN** ratios.

PM6:L8-BO:**2-MN**	V_{OC} [V]	J_{SC} [mA cm^{-2}]	FF [%]	PCE [%]
w/o	0.898	25.45	75.08	17.15
1:1.2:0.4	0.896	25.36	76.97	17.50
1:1.2:0.8	0.890	26.61	78.91	18.70
1:1.2:1.2	0.862	26.87	77.76	18.01
1:1.2:1.6	0.834	23.95	71.08	14.20

Table S4. Photovoltaic performance of the device with different **2,7-MN** ratios.

PM6:L8-BO:**2,7-MN**	V_{OC} [V]	J_{SC} [mA cm^{-2}]	FF [%]	PCE [%]
w/o	0.898	25.45	75.08	17.15
1:1.2:0.3	0.893	25.53	75.62	17.24
1:1.2:0.5	0.882	26.09	76.20	17.55
1:1.2:0.8	0.853	26.03	72.50	16.09

Table S5. The FF and PCE of some previously reported binary PSCs treated with non-halogenated solid additives.

Additives	FF[%]	PCE [%]	System	Ref.
DOB	75.60	17.05	PM6:L8-BO	[10]
DSB	73.90	15.59	PM6:L8-BO	[10]
IDT(BDT-IC)$_2$	71.24	16.34	PM6:Y6	[17]
2T	78.60	18.10	PM6:Y6	[14]
4T	76.80	17.20	PM6:Y6	[14]
9-FL	79.00	18.60	PM6:BTP-eC9	[7]
TOHA	76.20	17.91	D18-Cl:N3	[18]
BDT	77.11	17.91	PM6:Y6	[4]
ROPD	66.45	8.33	PTB7-Th:PC$_{71}$BM	[19]
DDO	70.09	10.10	BTR:PC$_{71}$BM	[20]
2-HM	79.40	18.85	PM6:L8-BO	[21]
2-MN(2-methoxynaphthalene)	76.40	17.32	PM6:PY-DT	[2]
TTA	73.46	15.80	PM6:BTP-eC9	[16]
TPA	77.65	17.30	PM6:BTP-eC9	[16]
DTB	70.50	14.50	PBDB-T:BO4Cl	[22]
Ph	77.82	18.47	D18-Cl:N3	[5]
DBT	79.33	18.87	PM6:L8-BO	[6]
NA	78.42	16.52	PM6:Y6	[1]

NDT	78.10	18.85	PM6:L8-BO	[23]
ADT	68.10	14.75	PM6:Y6	[23]
BTO	79.00	19.05	PM6:L8-BO	[24]
TT	75.10	17.75	PM6:Y6	[8]
SA-1	75.00	13.70	PBDB-TCl:IT-4F	[25]
SA-2	75.00	13.30	PBDB-TF:IT-4F	[25]
SA-3	75.00	13.20	PBDB-TF:IT-4F	[25]
SA-4	74.80	13.50	PBDB-TCl:IT-4F	[26]
SA-7	70.50	12.10	PBDB-TCl:IT-4F	[26]
SA-8	56.00	9.30	PBDB-TF:IT-4F	[25]
DTT-1	73.71	16.72	PM6:L15	[9]
DTT-2	77.26	18.72	PM6:L15	[9]
DTT-3	73.60	14.82	PM6:L15	[9]
Au:NCNT	71.78	9.45	PTB7:$PC_{70}BM$	[27]
Au:BCNT	72.09	9.81	PTB7:$PC_{70}BM$	[27]
GO-TPP	62.1	8.58	PTB7:$PC_{71}BM$	[28]
GO-TPP	58.4	6.92	PCDTBT:$PC_{71}BM$	[28]
N-GCD	71	8.6	PTB7:$PC_{71}BM$	[29]
BPQD	67.2	8.71	PTB7:$PC_{71}BM$	[30]
BPO	70.7	8.03	PTB7:$PC_{71}BM$	[12]
2,3-DHP	67	4.44	P3HT:$PC_{61}BM$	[31]
2,3-DHP	66	5.06	P3HT:$IC_{60}BA$	[32]
2-DHP	64	4.22	P3HT:$PC_{61}BM$	[33]
2,4-DHP	61	3,47	P3HT:$PC_{61}BM$	[33]
FCA	72.65	12.31	PBDB-T:IT-M	[34]
BP-BP	70.28	12.41	PBDB-T:ITIC	[35]
Fc	76	17.40	PM6:Y6	[15]
Bipy	69.44	8.73	J51:N2200	[13]
PID	74	15.9	PM6:Y6	[36]
M1	79.5	17.57	DAPor:6TIC	[37]
M2	77.1	16.70	DAPor:6TIC	[37]
2-MN	78.91	18.70	PM6:L8-BO	This work

Table S6. Relevant parameters obtained from the J_{ph}-V_{eff} Curve.

Additives	J_{sat} [mA cm^{-2}]	J_{ph} [mA cm^{-2}]	J_{max} [mA cm^{-2}]	J_{ph}/J_{sat}	J_{max}/J_{sat}
w/o	27.07	25.88	23.13	95.60%	85.45%
1-MN	27.04	26.26	24.19	97.12%	89.46%
2-MN	27.46	27.07	24.60	98.58%	89.58%
2,7-MN	27.16	26.20	24.04	96.47%	88.51%

Table S7. Contact angle, surface energy, and compatibility parameters for PM6 and L8-BO films under different conditions.

Films	Contact angle (deg)		γ	$\chi_{donor\text{-}acceptor}$
	H_2O	Eg	mN m^{-1}	
PM6	94.5	72.5	21.91	0.20
L8-BO	87.7	63.8	26.29	
PM6+**1-MN**	98.8	72.3	25.69	0.22
L8-BO+**1-MN**	91.5	62.5	30.69	
PM6+**2-MN**	97.5	69.4	28.18	0.07
L8-BO+**2-MN**	93.4	68.4	25.39	
PM6+**2,7-MN**	96.6	71.8	24.17	0.09
L8-BO+**2,7-MN**	90.5	71.3	21.31	

Table S8. The positions, *d*-spacing, FWHM, and CCL of the (010) and (100) peaks of the BHJ film with different additive treatments.

Blend films	Out-Of-plane π-π stacking cell long axis (010)				In-plane Unit cell long axis (100)			
	q	d-spacing	FWHM	CCL	q	d-spacing	FWHM	CCL
	[$Å^{-1}$]	[Å]	[$Å^{-1}$]	[Å]	[$Å^{-1}$]	[Å]	[$Å^{-1}$]	[Å]
PM6:L8-BO	1.500	4.188	0.307	20.47	0.283	22.175	0.075	84.34
PM6:L8-BO:**1-MN**	1.560	4.027	0.271	23.16	0.286	21.974	0.074	84.94
PM6:L8-BO:**2-MN**	1.545	4.066	0.271	23.22	0.285	22.063	0.071	87.95
PM6:L8-BO:**2,7-MN**	1.517	4.142	0.299	21.01	0.283	22.224	0.072	86.74

Table S9. The universality of **2-MN.**

Active layer	V_{OC} (V)	FF (%)	J_{SC} (mA cm^{-2})	PCE (%)

PTB7-Th:$PC_{71}BM$	0.809	54.22	16.12	7.07
PTB7-Th:$PC_{71}BM$:**2-MN**	0.807	68.09	17.91	9.84
PTB7-Th:IPY-T-IC	0.870	56.70	13.76	6.80
PTB7-Th:IPY-T-IC:**2-MN**[38]	0.830	55.50	16.51	7.68
PM6:PTer-N25	0.960	38.32	11.62	4.25
PM6:PTer-N25:**2-MN**[39]	0.940	65.13	19.52	11.94

References

[1] L. Zhong, S.-H. Kang, J. Oh, S. Jung, Y. Cho, G. Park, S. Lee, S.-J. Yoon, H. Park, C. Yang, *Adv. Funct. Mater.* 2022, 32, 2201080.

[2] J. Song, Y. Li, Y. Cai, R. Zhang, S. Wang, J. Xin, L. Han, D. Wei, W. Ma, F. Gao, Y. Sun, *Matter* 2022, 5, 4047-4059.

[3] Y. Ding, X. Zhang, H. Feng, X. Ke, L. Meng, Y. Sun, Z. Guo, Y. Cai, C. Jiao, X. Wan, C. Li, N. Zheng, Z. Xie, Y. Chen, *ACS Appl. Mater. Interfaces*, 2020, 12, 27425-27432.

[4] M. Dong, S. Chen, L. Hong, J. Jing, Y. Bai, Y. Liang, C. Zhu, T. Shi, W. Zhong, L. Ying, K. Zhang, F. Huang, *Nano Energy* 2024, 119, 109097.

[5] L. Zhong, Z. Sun, S. Lee, S. Jeong, S. Jung, Y. Cho, J. Park, J. Park, S.-J. Yoon, C. Yang, *Adv. Funct. Mater.* 2023, 33, 2305450.

[6] M. Xiao, L. Liu, Y. Meng, B. Fan, W. Su, C. Jin, L. Liao, F. Yi, C. Xu, R. Zhang, A.K.Y. Jen, W. Ma, Q. Fan, *Sci. China Chem.* 2023, 66, 1500-1510.

[7] L. Xu, Y. Xiong, S. Li, W. Zhao, J. Zhang, C. Miao, Y. Zhang, T. Zhang, J. Wu, S. Zhang, Q. Peng, Z. Wang, L. Ye, J. Hou, J. Wang, *Adv. Funct. Mater.* 2024, 34, 2314178.

[8] J. Chen, Y. Wang, L. Wang, F.R. Lin, C. Han, X. Ma, J. Zheng, Z. Li, J.A. Zapien, H. Gao, A.K.Y. Jen, *Small Methods* 2024, 9, 2400172.

[9] B. Liu, W. Xu, R. Ma, J.-W. Lee, T.A. Dela Peña, W. Yang, B. Li, M. Li, J. Wu, Y. Wang, C. Zhang, J. Yang, J. Wang, S. Ning, Z. Wang, J. Li, H. Wang, G. Li, B.J. Kim, L. Niu, X. Guo, H. Sun, *Adv. Mater.* 2023, 35, 2308334.

[10] T. Zhou, W. Jin, Y. Li, X. Xu, Y. Duan, R. Li, L. Yu, Q. Peng, *Adv. Sci.* 2024, 11, 2401405.

[11] Z. Chen, H. Yao, J. Wang, J. Zhang, T. Zhang, Z. Li, J. Qiao, S. Xiu, X. Hao, J. Hou, *Energy Environ. Sci*. 2023, 16, 2637-2645.

[12] P. Cheng, C. Yan, T.K. Lau, J. Mai, X. Lu, X. Zhan, *Adv. Mater.* 2016, 28, 5822-5829.

[13] Y. Yan, Y. Liu, J. Zhang, Q. Zhang, Y. Han, *J. Mater. Chem. C* 2021, 9, 3835-

3845.
[14] W. Liang, L. Chen, Z. Wang, Z. Peng, L. Zhu, C.H. Kwok, H. Yu, W. Xiong, T. Li, Z. Zhang, Y. Wang, Y. Liao, G. Zhang, H. Hu, Y. Chen, *Adv. Energy Mater.* 2024, 2303661.
[15] L. Ye, Y. Cai, C. Li, L. Zhu, J. Xu, K. Weng, K. Zhang, M. Huang, M. Zeng, T. Li, E. Zhou, S. Tan, X. Hao, Y. Yi, F. Liu, Z. Wang, X. Zhan, Y. Sun, *Energy Environ. Sci.* 2020, 13, 5117-5125.
[16] R. Yu, R. Shi, Z. He, T. Zhang, S. Li, Q. Lv, S. Sha, C. Yang, J. Hou, Z.a. Tan, *Angew. Chem. Int. Ed.* 2023, 62, e202308367.
[17] R. Lin, H. Zhou, X. Xu, X. Ouyang, *Surfaces and Interfaces* 2024, 46, 104072.
[18] H. Kang, Y. Jing, Y. Zhang, Y. Li, H. Zhang, H. Zhou, Y. Zhang, *Solar RRL* 2023, 7, 2201084.
[19] Q. Zhang, C. Bao, S. Cui, P. Zhong, K. Zhang, W. Zhu, Y. Liu, *J. Mater. Chem. C* 2020, 8, 16551-16560.
[20] X. Du, X. Li, H. Lin, L. Zhou, C. Zheng, S. Tao, *J. Mater. Chem. A* 2019, 7, 7437-7450.
[21] X. Yang, B. Li, X. Zhang, S. Li, Q. Zhang, L. Yuan, D.-H. Ko, W. Ma, J. Yuan, *Adv. Mater.* 2023, 35, 2301604.
[22] R. Yu, H. Yao, Y. Xu, J. Li, L. Hong, T. Zhang, Y. Cui, Z. Peng, M. Gao, L. Ye, Z. Tan, J. Hou, *Adv. Funct. Mater.* 2021, 31, 2010535.
[23] W. Zhang, Y. Wu, R. Ma, H. Fan, X. Li, H. Yang, C. Cui, Y. Li, *Angew. Chem. Int. Ed.* 2023, 62, e202309713.
[24] M. Xiao, Y. Meng, L. Tang, P. Li, L. Tang, W. Zhang, B. Hu, F. Yi, T. Jia, J. Cao, C. Xu, G. Lu, X. Hao, W. Ma, Q. Fan, *Adv. Funct. Mater.* 2024, 34, 2311216.
[25] R. Yu, H. Yao, L. Hong, Y. Qin, J. Zhu, Y. Cui, S. Li, J. Hou, *Nat. Commun.* 2018, 9, 4645.
[26] R. Yu, H. Yao, Z. Chen, J. Xin, L. Hong, Y. Xu, Y. Zu, W. Ma, J. Hou, *Adv. Mater.* 2019, 31, 1900477.
[27] J.M. Lee, J. Lim, N. Lee, H.I. Park, K.E. Lee, T. Jeon, S.A. Nam, J. Kim, J. Shin, S.O. Kim, *Adv. Mater.* 2014, 27, 1519-1525.

[28] M.M. Stylianakis, D. Konios, G. Kakavelakis, G. Charalambidis, E. Stratakis, A.G. Coutsolelos, E. Kymakis, S.H. Anastasiadis, *Nanoscale* 2015, 7, 17827-17835.

[29] B.J. Moon, Y. Oh, D.H. Shin, S.J. Kim, S.H. Lee, T.-W. Kim, M. Park, S. Bae, *Chem. Mater.* 2016, 28, 1481-1488.

[30] S. Liu, S. Lin, P. You, C. Surya, S.P. Lau, F. Yan, *Angew. Chem. Int. Ed.* 2017, 56, 13717-13721.

[31] C.-G. Wu, C.-H. Chiang, H.-C. Han, *J. Mater. Chem. A* 2014, 2, 5295-5303.

[32] B. Xu, G. Sai-Anand, A.-I. Gopalan, Q. Qiao, S.-W. Kang, *Polymers*, 2018, 10, 121.

[33] B. Xu, G. Sai-Anand, G.E. Unni, H.-M. Jeong, J.-S. Kim, S.-W. Kim, J.-B. Kwon, J.-H. Bae, S.-W. Kang, *Appl. Surface Sci.* 2019, 484, 825-834.

[34] Q. Guo, Y. Liu, M. Liu, H. Zhang, X. Qian, J. Yang, J. Wang, W. Xue, Q. Zhao, X. Xu, W. Ma, Z. Tang, Y. Li, Z. Bo, *Adv. Mater.* 2020, 32, 2003164.

[35] P. Fan, W. Sun, X. Zhang, Y. Wu, Q. Hu, Q. Zhang, J. Yu, T.P. Russell, Adv. Funct. Mater. 2021, 31, 2008699.

[36] M. Choi, H.-S. Jeong, J. Lee, Y. Choi, I.-B. Kim, D.-Y. Kim, H. Kang, S.-Y. Jang, *J. Mater. Chem. A* 2024, 12, 8963-8971.

[37] Y. Miao, Y. Sun, W. Zou, X. Zhang, Y. Kan, W. Zhang, X. Jiang, X. Wang, R. Yang, X. Hao, L. Geng, H. Xu, K. Gao, *Adv. Mater.* 2024, 36, 2406623.

[38] L. Chen, M. Zeng, C. Weng, S. Tan, P. Shen, *ACS Appl. Mater. Interfaces* 2019, 11, 48134-48146.

[39] H. Liu, L. Wang, H. Liu, M. Guan, C.-J. Su, U.S. Jeng, B. Zhao, C. Weng, K. You, X. Lu, *Chem. Eng. J.* 2022, 429, 132407.